Supplementary Material: *Ab initio* Quantum Monte Carlo simulation of the warm dense electron gas in the thermodynamic limit

Tobias Dornheim[1], Simon Groth[1], Travis Sjostrom[2], Fionn D. Malone[3], W.M.C. Foulkes[3], and Michael Bonitz[1]

[1]Institut für Theoretische Physik und Astrophysik, Christian-Albrechts-Universität zu Kiel, D-24098 Kiel, Germany
[2]Theoretical Division, Los Alamos National Laboratory, Los Alamos, New Mexico 87545, USA
[3]Department of Physics, Imperial College London, Exhibition Road, London SW7 2AZ, UK

A. Static structure factors

In Fig. S1, as a supplement to Fig. 2 of the main manuscript, we show the structure factors (SF) at $\theta = 2$ for intermediate ($r_s = 1$) and lower ($r_s = 10$) density. At both densities the STLS structure factor smoothly connects to the QMC data but exhibits significant deviations at larger k. The low k expansion of the RPA SF fails to connect to the QMC data at $r_s = 1$, indicating that the FSC by Brown *et al.* is inappropriate, while at $r_s = 10$ the RPA expansion smoothly connects to the QMC data so that the FSC by Brown *et al.* is applicable.

B. Practical details

For the evaluation of the discretization error (DE) according to Eq. (5) in the main manuscript,

$$\frac{\Delta V_N}{N}(G_{\max}) = 2\pi\Bigg(\int_{k<G_{\max}} \mathrm{d}\mathbf{k}\, \frac{S_{\text{model}}(k)-1}{k^2(2\pi)^3} - \sum_{\mathbf{G}\neq\mathbf{0}}^{G_{\max}} \frac{S_{\text{model}}(\mathbf{G})-1}{G^2 V} - \xi_{\text{M}} \Bigg) \quad , \tag{S.1}$$

the maximum modulus of the discrete lattice vectors $G_{\max}$ has to be chosen large enough to ensure the convergence of the FSC, which is demonstrated in Fig. S2 for three different particle numbers at $\theta = 2$ and $r_s = 0.5$. Clearly, taking into account only the first k-vector is not sufficient. In fact, the convergence of the DE with respect to $G_{\max}$ is rather slow, and the number of k-vectors needed for convergence of the DE only weakly depends on N. The difference between the converged values is due to the different k-mesh for different N.

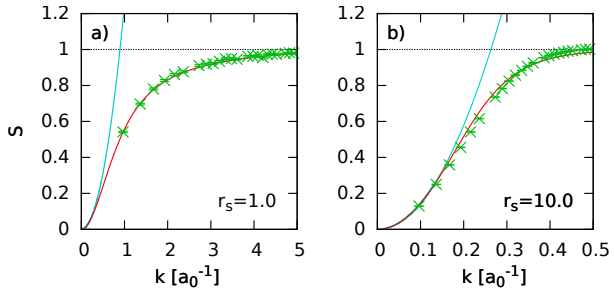

Figure S1: Static structure factors of $N = 66$ electrons at $\theta = 2$ for a) $r_s = 1.0$ and b) $r_s = 10.0$: QMC data (green crosses), STLS (red) and $k \to 0$ expansion of the the RPA SF (light blue).

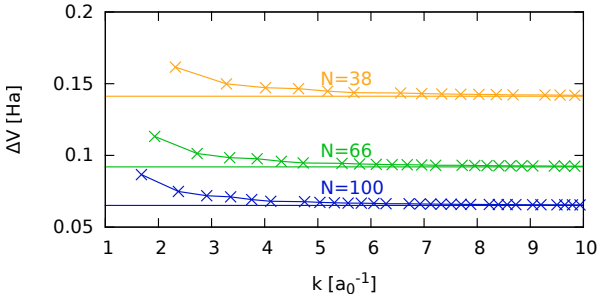

Figure S2: Convergence of the FSC with the maximum k-value for three particle numbers and $\theta = 2$ and $r_s = 0.5$, cf. Fig. 3 in the main manuscript.

C. Finite-size corrections for selected parameters

To demonstrate the broad range of applicability of our finite size correction (FSC) procedure, we present some more examples for different parameter combinations. Figure S3 shows the convergence of the potential energy with system size for the most challenging (with respect to finite-size errors) case at $\theta = 8$ and $r_s = 0.1$. Evidently, the uncorrected QMC (CPIMC) data exhibit severe finite-size errors of $\Delta V/V \approx 200\%$ for $N = 34$. This is a direct consequence of the steep drop of the static structure factor $S(k)$ at small k, that is not properly accessed by the available k-values even in a QMC simulation of $N = 1000$ electrons. Further, the potential energy that is obtained by invoking the BCDC-FSCs even worsens the convergence, as $S_0^{\text{RPA}}(k)$ does not come anywhere near the QMC-data, even for $N = 1000$. In striking contrast, our FSCs (using either S^{STLS}, or a combination of STLS with the QMC data, S_{comb}) are converged to a remarkably high degree, even for relatively small systems (with $|\Delta V|/|V| \sim 10^{-3}$, for $N = 66$) and the additional extrapolation of the residual finite-size errors allows for an accurate result for V in the TDL even for such extreme parameters.

Figure S4 shows the convergence for $\theta = 2$ and $r_s = 1$. In this case, the uncorrected QMC (permutation blocking PIMC) data exhibit finite-size errors of $|\Delta V|/|V| \approx 10\%$

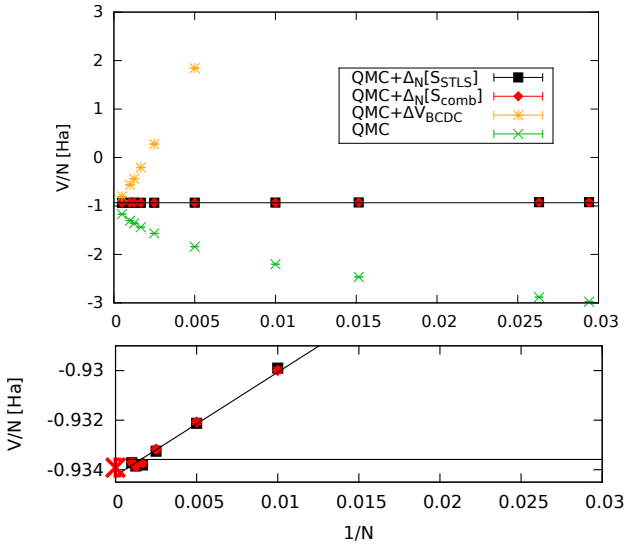

Figure S3: Finite-size correction of the QMC results for the potential energy with $\theta = 8$ and $r_s = 0.1$.

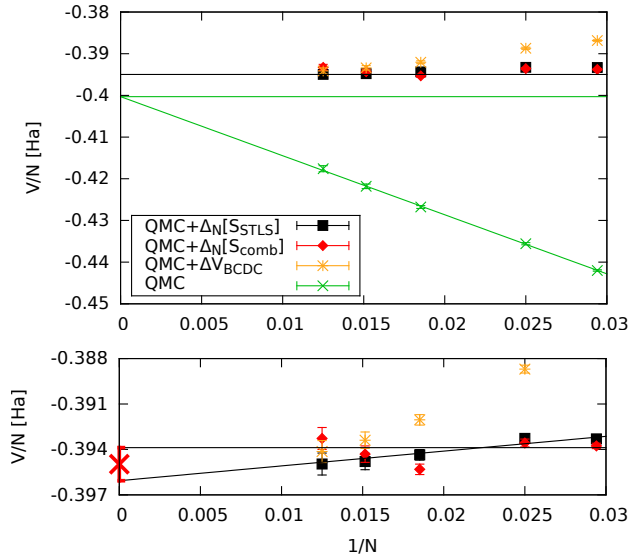

Figure S4: Same as Fig. S3, but for $\theta = 2$ and $r_s = 1$.

(for $N = 34$) and the convergence seems to follow $|\Delta V|/N \sim 1/N$, cf. the linear fit (the green line). Although, in principle, the $1/N$-behavior is predicted by the BCDC-FSCs, the slope is different and the corrected V/N-data do not agree with the linear extrapolation and are not converged. The data that have been obtained after adding our new FSCs are converged to a high degree, but do not agree with the linearly extrapolated value as well. This, again, clearly demonstrates the danger of a direct extrapolation of the QMC data without being certain about the exact functional form of the finite-size error.

D. Fit of the potential energy

Following Karasiev *et al.* [1], we use the following parametrization of the exchange-correlation free energy for fixed θ:

$$\frac{F_{xc}}{N}(r_s,\theta) = -\frac{1}{r_s}\left(\frac{a + b\sqrt{r_s} + cr_s}{1 + d\sqrt{r_s} + er_s}\right) \quad , \tag{S.2}$$

which yields the potential energy via

$$V(r_s,\theta)r_s = 2r_s F_{xc}(r_s,\theta) + r_s^2 \frac{\partial F_{xc}(r_s,\theta)}{\partial r_s}\bigg|_\theta \quad , \tag{S.3}$$

which allows us to fit the rhs. of Eq. (S.3) to our new corrected QMC data. The parameter a follows from the Hartree-Fock limit and the results of the fit procedure for the five isotherms shown in Fig. 4 in the main article are listed in table I.

E. STLS and RPA

The static structure factor (SF) is found by the fluctuation-dissipation theorem as a sum over the Matsubara frequencies for the polarizabilities of the interacting system as

$$S(\mathbf{k}) = \frac{-1}{\beta n}\sum_{l=-\infty}^{\infty}\frac{1}{v_k}\left(\frac{1}{\epsilon(\mathbf{k},z_l)} - 1\right) \quad , \tag{S.4}$$

with the particle density n, the Matsubara frequencies $z_l = 2\pi i l/\beta\hbar$, and the Fourier transform of the Coulomb potential $v_k = 4\pi/k^2$. Following [2], the Singwi-Tosi-Land-Sjölander (STLS) SF is computed from the dielectric function

$$\epsilon(\mathbf{k},\omega) = 1 - \frac{v_k\chi_0(\mathbf{k},\omega)}{1 + G(\mathbf{k})v_k\chi_0(\mathbf{k},\omega)} \quad , \tag{S.5}$$

with $\chi_0(\mathbf{q},\omega)$ being the finite-temperature polarizability of the non-interacting UEG, G is the static local field correction

$$G(\mathbf{k}) = \frac{-1}{n}\int\frac{\mathrm{d}\mathbf{k}'}{(2\pi)^3}\frac{\mathbf{k}\cdot\mathbf{k}'}{k'^2}[S(\mathbf{k}-\mathbf{k}') - 1], \tag{S.6}$$

and Eq. (S.4), (S.5), and (S.6) are solved self-consistently. In the random phase approximation (RPA), $G(\mathbf{k}) \to 0$.

F. Finite-size corrections by Brown *et al.*

In Fig. 4 from the main manuscript, we have compared our new corrected data for the potential energy to RPIMC data (for $N = 66$) by Brown *et al.* that were corrected with the BCDC-FSC [Eq. (4) of the main article]. However, it should be noted that this corrected data differs from the data tabulated in the supplement of Ref. [3].

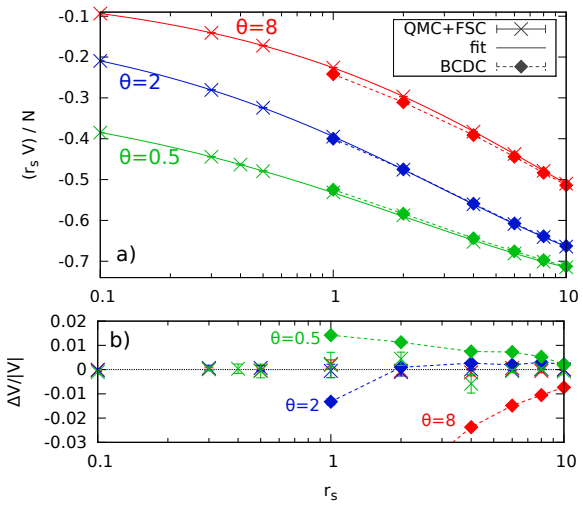

Figure S5: Potential energy of the warm dense electron gas in the TDL. Panel **a)** shows our new corrected data for three temperatures, the fits to our data (see Eq. (S.3)), and the data by Brown *et al.* (BCDC), taken directly from their supplement. Panel **b)** shows the corresponding relative deviations to the fits to our data.

For the latter, apparently, there was a problem caused by a mix of Hartree and Rydberg atomic units within their FSC. In Fig. S5, we compare our data to the BCDC results as they are given in their supplement. While the magnitude of the deviation is similar as in Fig. 4 from the main article, the sign changes with temperature. In particular, for $\theta = 8$ the BCDC values are lower by $\Delta V/V \approx 8\%$ than ours instead of being too high, and the two data sets significantly disagree even for $r_s = 10$.

G. Data

As a supplement to Fig. 4 from the main article, we have listed all data for the potential and exchange correlation free energy of the macroscopic UEG in Table II.

[1] V.V. Karasiev, T. Sjostrom, J. Dufty and S.B. Trickey, Accurate Homogeneous Electron Gas Exchange-Correlation Free Energy for Local Spin-Density Calculations, *Phys. Rev. Lett.* **112**, 076403 (2014)

[2] S. Tanaka and S. Ichimaru, Thermodynamics and Correlational Properties of Finite-Temperature Electron Liquids in the Singwi-Tosi-Land-Sjölander Approximation, *J. Phys. Soc. Jpn.* **55**, 2278-2289 (1986)

[3] E.W. Brown, B.K. Clark, J.L. DuBois and D.M. Ceperley, Path-Integral Monte Carlo Simulation of the Warm Dense Homogeneous Electron Gas, *Phys. Rev. Lett.* **110**, 146405 (2013)

Table I: Fit parameters from Eq. (S.3), see Fig. 4 in the main article.

θ	a	b	c	d	e
8.0	0.025 26	0.151 46	0.015 624	0.158 37	0.021 73
4.0	0.049 81	0.216 40	0.046 744	0.315 83	0.054 29
2.0	0.095 88	0.302 37	0.081 005	0.454 80	0.093 17
1.0	0.173 85	0.389 00	0.097 468	0.554 82	0.113 88
0.5	0.278 86	0.404 12	0.054 329	0.519 84	0.063 44

Table II: Energies per particle of the warm dense electron gas in the thermodynamic limit: Listed are the potential energy V/N (finite-size corrected QMC data where the residual error has been removed by an additional extrapolation, cf. Fig. 3 in the main article), the corresponding uncertainty $\delta V/N$ and the exchange correlation free energy F_{xc}/N that has been obtained by the fit, see Sec. D.

θ	r_s	V/N	$\delta V/N$	F_{xc}/N
8.0	10.0	−0.051 01	0.000 02	−0.038 442
8.0	8.0	−0.059 84	0.000 04	−0.044 601
8.0	6.0	−0.072 91	0.000 05	−0.053 789
8.0	4.0	−0.0956	0.0001	−0.069 583
8.0	2.0	−0.1483	0.0002	−0.106 794

Table II: *(continued).*

θ	r_s	V/N	$\delta V/N$	F_{xc}/N
8.0	1.0	−0.2259	0.0004	−0.162 990
8.0	0.5	−0.3442	0.000 19	−0.249 668
8.0	0.3	−0.4692	0.0003	−0.344 241
8.0	0.1	−0.9341	0.0003	−0.710 052
4.0	10.0	−0.059 74	0.000 01	−0.047 280
4.0	6.0	−0.088 43	0.000 02	−0.068 305
4.0	4.0	−0.119 06	0.000 04	−0.090 529
4.0	2.0	−0.1929	0.0004	−0.144 405
4.0	1.0	−0.3060	0.0003	−0.228 337
4.0	0.5	−0.4811	0.0003	−0.361 760
4.0	0.3	−0.6722	0.0003	−0.511 220
4.0	0.1	−1.4091	0.0007	−1.112 758
2.0	10.0	−0.066 409	0.000 003	−0.055 243
2.0	8.0	−0.080 093	0.000 009	−0.065 910
2.0	6.0	−0.101 461	0.000 014	−0.082 412
2.0	4.0	−0.140 11	0.000 03	−0.112 123
2.0	2.0	−0.2380	0.0004	−0.187 073
2.0	1.0	−0.3950	0.0011	−0.309 220
2.0	0.5	−0.6484	0.0007	−0.511 632
2.0	0.3	−0.9350	0.0010	−0.746 033
2.0	0.1	−2.0956	0.0013	−1.732 828
1.0	10.0	−0.070 264	0.000 014	−0.061 098
1.0	8.0	−0.085 593	0.000 009	−0.073 774
1.0	6.0	−0.109 94	0.000 04	−0.093 763
1.0	4.0	−0.155 37	0.000 10	−0.130 733
1.0	2.0	−0.2749	0.0003	−0.228 179
1.0	1.0	−0.4769	0.0005	−0.395 507
1.0	0.5	−0.8225	0.0011	−0.686 721
1.0	0.3	−1.2301	0.0010	−1.037 072
1.0	0.1	−2.972	0.003	−2.585 960
0.5	10.0	−0.071 47	0.000 10	−0.064 069
0.5	8.0	−0.087 60	0.000 04	−0.077 981
0.5	6.0	−0.113 52	0.000 08	−0.100 212
0.5	4.0	−0.1631	0.0006	−0.142 231
0.5	2.0	−0.2938	0.0008	−0.257 459
0.5	1.0	−0.531	0.003	−0.465 543
0.5	0.5	−0.959	0.003	−0.845 752
0.5	0.4	−1.158	0.002	−1.026 811
0.5	0.3	−1.4808	0.0011	−1.320 709
0.5	0.1	−3.851	0.004	−3.521 367